# Autocorrelation and Cross-Correlation of MHD Turbulence across IP Shock: Multispacecraft Analysis


Ilyas Abushzada [1], Alexander Pitna [1], Zdenek Nemecek [1] and Jana Safrankova [1]

[1] Charles University, Faculty of Mathematics and Physics, Prague, Czech Republic


Hall X4, X4.158

## Abstract


One of the key processes in the solar wind is turbulence, which has an effect on plasma fluctuations, governs energy transfer within the heliosphere, and drives particle acceleration. In this study, we aim to investigate the nature of large- and small-scale fluctuations in the upstream and downstream regions of interplanetary (IP) shocks. By analyzing magnetic field fluctuations using autocorrelation (ACF) and cross-correlation functions (CCF), we examine changes in correlation length, Taylor scale, and effective Reynolds number from upstream to downstream regions. For this investigation we use data from ACE, Wind and DSCOVR missions. Analysis of the Reynolds number shows a decrease in values when moving from upstream to downstream regions, suggesting turbulence resetting in the case under consideration. Building on the findings of a case study, we will extend our investigations by performing a statistical analysis of these parameters in other interplanetary shocks.


## Turbulence and Interplanetary (IP) Shock

Magnetohydrodynamic (MHD) turbulence refers to the complex interactions between magnetic fields and plasma flows, resulting in chaotic and dynamic behavior. In this context, IP shocks are discontinuities that occur due to the nonlinear steepening of waves. The characteristics of these shocks include their type (fast or slow), obliquity (whether they are parallel, perpendicular, or oblique), the direction of their travel, and their classification based on their causes.

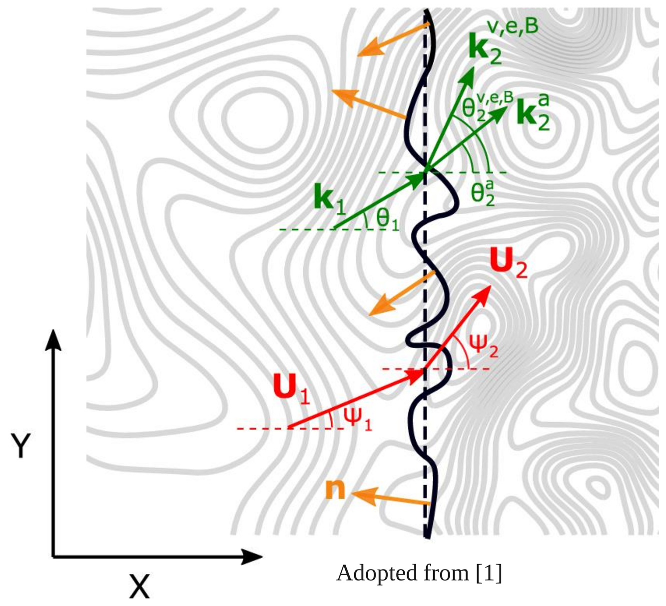


Fig. 1. Schematic representation of MHD turbulence and shock interactions.

The figure shows shock wave in presence of magnetic islands in upstream (1) and downstream (2) regions. The equation below describes the relationship between the upstream and downstream wave numbers. $\theta_1$ and $\theta_2$ mark the angle between shock normal and upstream and downstream wavevector $k_1$ and $k_2$, respectively

$$k_2 = R_B \frac{\cos\theta_1}{\cos\theta_2} k_1 \Longrightarrow \begin{cases} \theta_1 = \theta_2 = 90^o \Longrightarrow k_2 = k_1 \\ \theta_1 = \theta_2 = 0^o \Longrightarrow \boxed{k_2 = R_B k_1} \end{cases}$$

## Methodology

The correlation function of the magnetic field fluctuations which for stationary and homogeneous turbulence is a function only of the spatial lag r. Here angle brackets denote a suitable time average

$$R(\mathbf{r}) = \langle \mathbf{b}(\mathbf{x}) \cdot \mathbf{b}(\mathbf{x}+\mathbf{r}) \rangle \xrightarrow[\tau = \frac{\lambda}{v_{sw}}]{} \boxed{R(\tau) = \frac{\langle \mathbf{b}(t) \cdot \mathbf{b}(t+\tau) \rangle}{\langle \mathbf{b}^2 \rangle}} \quad \mathbf{b}(t) = \mathbf{B}(t) - \langle \mathbf{B}(t) \rangle$$

In our work, we apply the Taylor hypothesis, which states that temporal changes measured by the spacecraft reflect spatial plasma structures in the bulk flow. After calculating the ACF, we determine the correlation length ($\lambda_C$). To find the effective Reynolds number, a key parameter for describing turbulent processes, we calculated the Taylor microscale ($\lambda_T$), which represents the scale at which viscous effects begin to influence the turbulent motion, but are not yet dominant.

$$\boxed{ACF(\lambda) = 1 - \frac{\lambda^2}{2 \cdot \lambda_T^2}}$$

The solar wind lacks a well-defined viscosity, so the Reynolds number cannot be directly determined. Therefore, we estimate effective Reynolds number

$$\boxed{Re_{eff} = \left(\frac{\lambda_C}{\lambda_T}\right)^2}$$

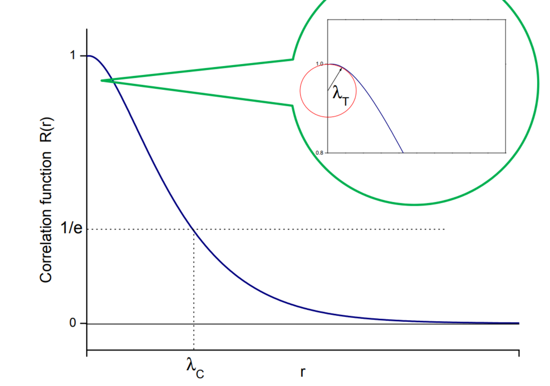


Fig. 2. Schematic diagram of the autocorrelation function as a function of distance.

## Data

**01.07.2017**

Table 1

| Time | Spc | $B^{down}/B^{up}$ | $T^{down}/T^{up}$ | $v^{down}/v^{up}$ | $\beta_{up}$ | $\theta_{Bn}$ |
|---|---|---|---|---|---|---|
| 16:34:14 | WIND | 1.60 | 1.27 | 1.12 | 0.4 | 86 |
| 16:26:40 | DSCOVR | 1.63 | 1.44 | 1.12 | 0.5 | 85 |
| 16:21:15 | ACE | 1.63 | 1.4 | 1.13 | 0.5 | 78 |

Why we choose this interval? It features well-defined interplanetary shock observed by all three spacecraft, allowing for consistent analysis.

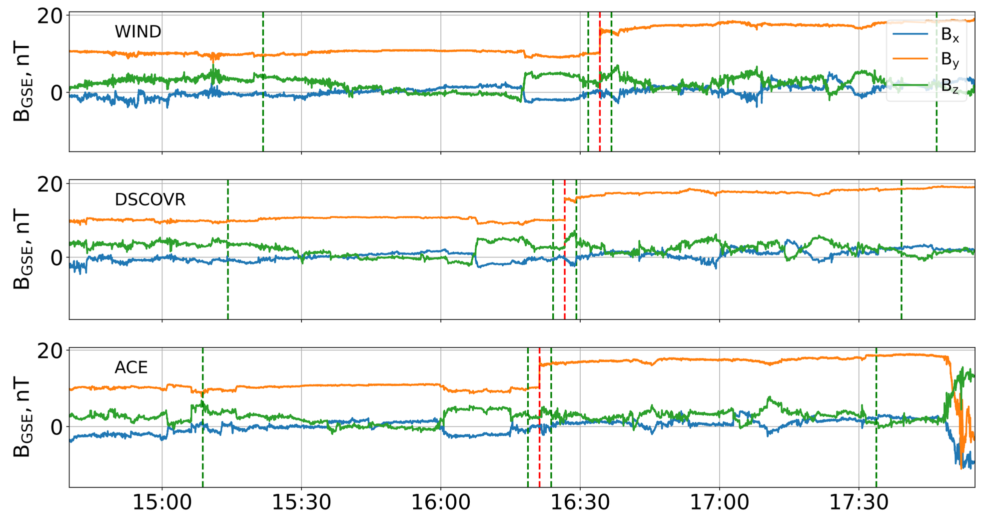


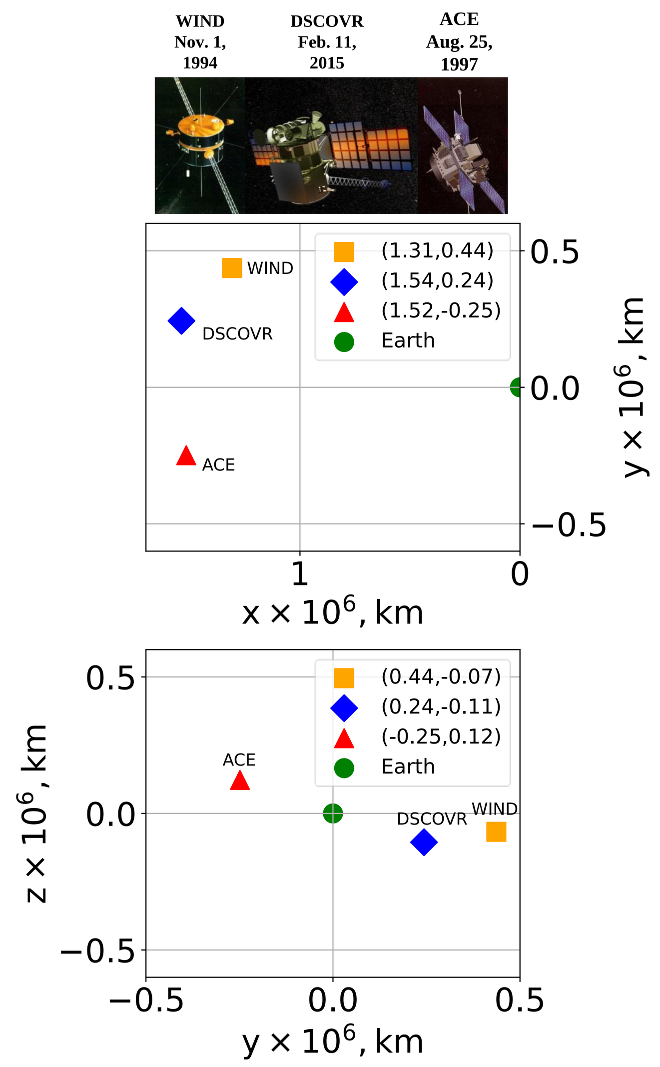


Fig. 3. Time evolution of magnetic field components from three spacecraft missions and their corresponding positions projected onto the XY and YZ planes in the Geocentric Solar Ecliptic (GSE) coordinate system.

## Autocorrelation function (ACF)

The Taylor hypothesis was used to convert the horizontal axis from time to spatial lag. The figures show autocorrelation functions (ACFs) for Wind, DSCOVR, and ACE spacecraft upstream and downstream (70 minutes).

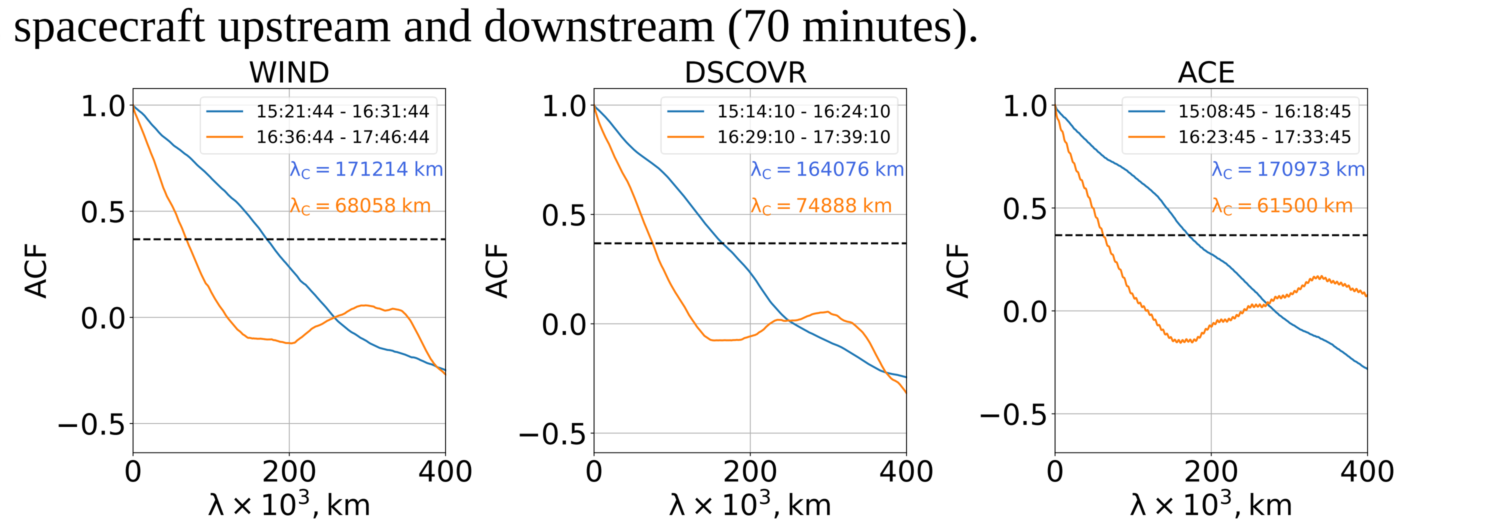


Fig. 4. ACFs showing the upstream region in blue and the downstream region in orange, where $\lambda$ is the spatial lag.

Table 2

| $\lambda_C$, km | Upstream | Downstream | $\frac{\lambda^{up}}{\lambda^{down}}$ |
|---|---|---|---|
| Wind | 171214 | 68058 | 2.52 |
| DSCOVR | 164076 | 74888 | 2.19 |
| ACE | 170973 | 61500 | 2.78 |

$$ACF(\tau) = \frac{\sum_{t=1}^{N-\tau} (\mathbf{B}_t - \langle \mathbf{B} \rangle)(\mathbf{B}_{t+\tau} - \langle \mathbf{B} \rangle)}{\sum_{t=1}^{N} (\mathbf{B}_t - \langle \mathbf{B} \rangle)^2}$$

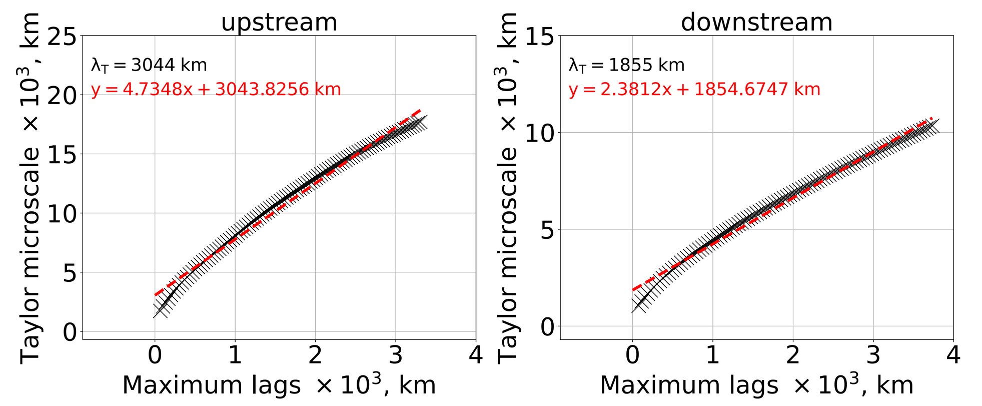


Fig. 5. $\lambda_T$ estimation in upstream and downstream based on extrapolation.

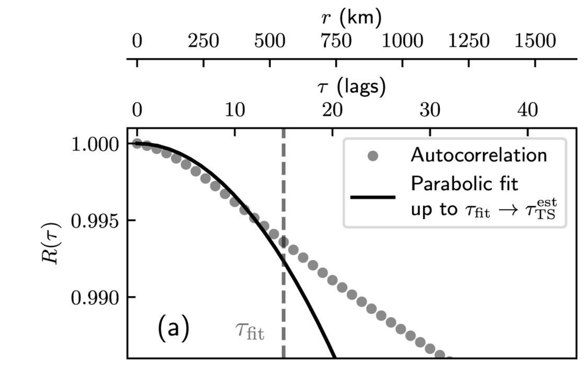


The Taylor microscale has been estimated by fitting a parabola to the origin of the ACF. This was done by fitting the parabola over increasing numbers of points near the origin, ranging from 2 to 100. These are shown as Taylor microscale vs. maximum lag. The output was extrapolated to zero lag to optimize measurement accuracy. Wind gives better estimate due to the high resolution of data.

The $Re_{eff}$ is higher in the upstream region.

To compare our observational results with the already known theoretical predictions, we show the ratio of the power spectral density (PSD) of the magnetic field in the downstream and upstream regions. In the right figure, the bold line represents the ratio obtained from observations, while the thin line shows the theoretical ratio. The average ratio $R_{ot}$ of **o**bserved and **t**heoretically predicted downstream PSD yields $R_{ot} = 0.73$

| Upstream | WIND |
|---|---|
| $\lambda_C$, km | 170000 |
| $\lambda_T$, km | 3000 |
| $Re_{eff}$ | 3200 |

| Downstream | WIND |
|---|---|
| $\lambda_C$, km | 68000 |
| $\lambda_T$, km | 2000 |
| $Re_{eff}$ | 1200 |

Table 3

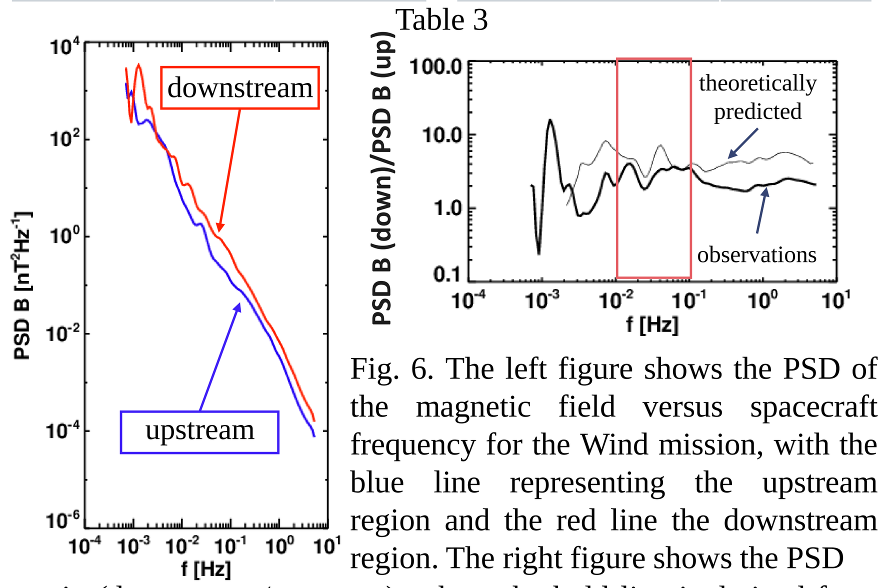


Fig. 6. The left figure shows the PSD of the magnetic field versus spacecraft frequency for the Wind mission, with the blue line representing the upstream region and the red line the downstream region. The right figure shows the PSD ratio (downstream/upstream), where the bold line is derived from observations and the thin line represents the theoretical prediction.

## Cross-correlation function (CCF)

To calculate the cross-correlation function, we applied time shifting and identified the peak values of the correlation function. In the downstream region, two peaks were observed; however, we selected the second peak as the most relevant, as the magnetic field data suggested that the magnetic field variations were nearly identical over time.

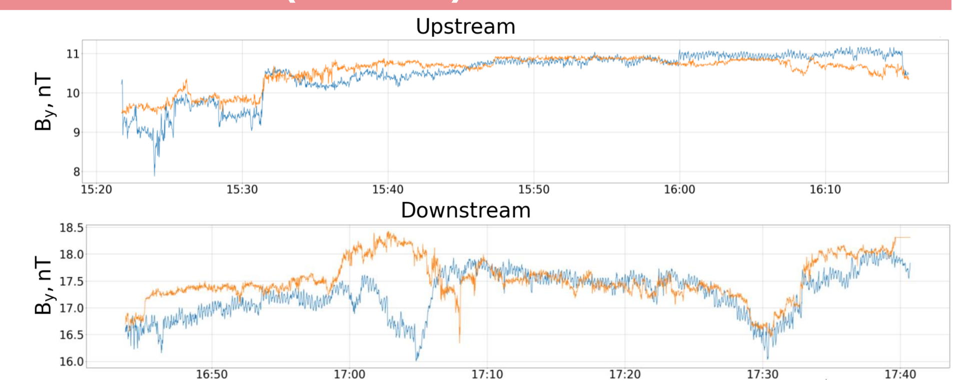


Fig. 7. Y component of the magnetic field, where the Wind data is represented in orange and the ACE data in blue in upstream and downstream regions.

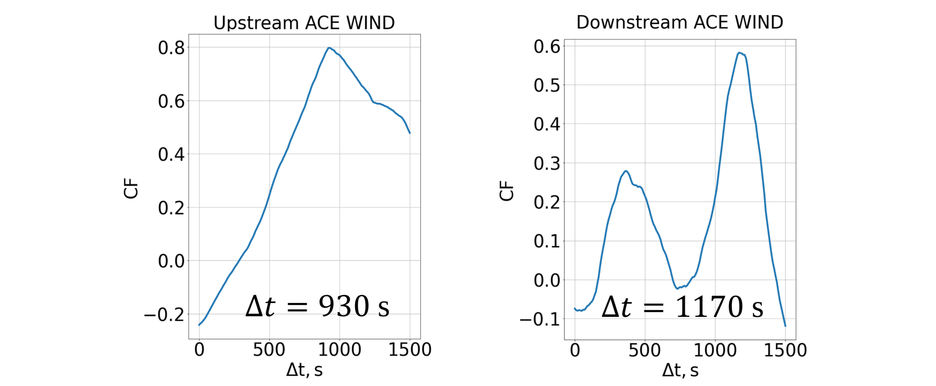


Fig. 8. The figures show the cross-correlation function as a function of the time by which the data were shifted (Δt)

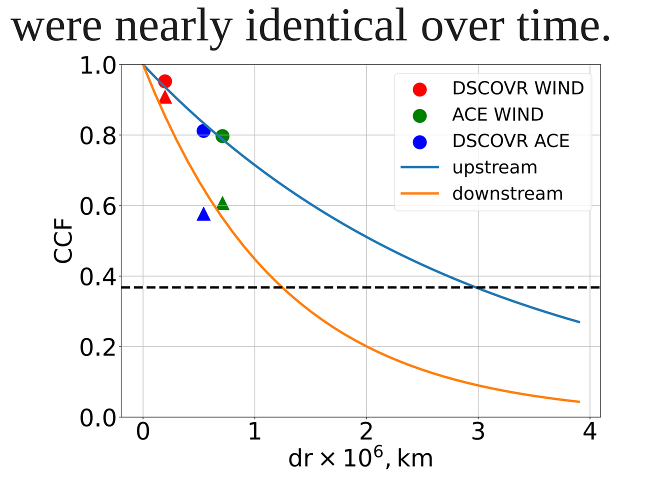


Fig. 9. Cross-correlation function vs inter-spacecraft distance in the YZ plane, with fits applied to upstream and downstream regions.

$$\boxed{CCF = e^{-\frac{\lambda}{\lambda_C}}}$$

| | |
|---|---|
| $\lambda_C^{up} \cdot 10^6$, km | 2.98 |
| $\lambda_C^{down} \cdot 10^6$, km | 1.25 |
| $\frac{\lambda_C^{up}}{\lambda_C^{down}}$ | 2.38 |

Table 4

## Discussion and Conclusion

- The study shows differences in turbulent characteristics between the upstream and downstream regions of interplanetary (IP) shocks, as observed through multi-spacecraft data analysis.
- Ratio of $\lambda_C$ obtained from the correlation function (Tab. 2) and cross-correlation functions (Tab. 4) are different from the theoretical prediction due to the small interval chosen for the calculations.
- The ACF in the downstream region appears more consistent, as the one-hour interval used downstream corresponds approximately to a five-hour interval of data upstream.
- Multi-spacecraft analysis was used to calculate the correlation length from cross-correlation functions (CCFs).
- The correlation length calculated from the CCF (Tab. 4) is significantly larger than that from the ACF (Tab. 2); however, the ratio between them is the same.
- The following parameters decrease from the upstream to the downstream region: correlation length ($\lambda_C$), Taylor microscale ($\lambda_T$), effective Reynolds number ($Re_{eff}$) (Tab. 3)
- The ratio between observed and predicted PSD is consistent with previous findings [4]

### Acknowledgements


The present work is supported by the Czech Science Foundation under contract 23-06401S, the Charles University Grant Agency under contract 280423 and the MSMT grant LUAUS25060. The authors thank all Wind, DSCOVR, and ACE teams for the magnetic field and plasma data.


### References


[1] G. P. Zank et al 2021 ApJ **913** 127
[2] R. Bruno et al 2013 Living Rev. Sol. Phys. 10, 2.
[3] D. Wrench et al 2024 ApJ 961 182
[4] A. Pitňa et al 2017 ApJ 844 51